<u>10RU 2001</u>

Multi-TeV gamma-ray observation of several strong outbursts of Mrk 421 during 2000 and 2001 with the Tibet-III air-shower array

The Tibet AS γ Collaboration

M. Amenomori¹, S. Ayabe², S.W. Cui³, L.K. Ding³, X.Y. Ding⁴, C.F. Feng⁵, Z.Y. Feng⁶, Y. Fu⁵, X.Y. Gao⁷, Q.X. Geng⁷, H.W. Guo⁴, M. He⁵, K. Hibino⁸, N. Hotta⁹, J. Huang⁹, Q. Huang⁶, A.X. Huo³, K. Izu¹⁰, H.Y. Jia⁶, F. Kajino¹¹, K. Kasahara¹², Y. Katayose¹³, K. Kawata¹¹, Labaciren⁴, G.M. Le¹⁴, J.Y. Li⁵, H. Lu³, S.L. Lu³, G.X. Luo³, X.R. Meng⁴, K. Mizutani², J. Mu⁷, H. Nanjo¹, M. Nishizawa¹⁵, M. Ohnishi¹⁰, I. Ohta⁹, T. Ouchi¹⁰, S. Ozawa⁹, J.R. Ren³, T. Saito¹⁶, M. Sakata¹¹, T. Sasaki⁸, M. Shibata¹³, A. Shiomi¹⁰, T. Shirai⁸, H. Sugimoto¹⁷, K. Taira¹⁷, M. Takita¹⁰, Y.H. Tan³, N. Tateyama⁸, S. Torii⁸, H. Tsuchiya¹⁰, S. Udo², T. Utsugi², C.R. Wang⁵, H. Wang³, X. Wang⁵, X.W. Xu^{3,10}, L. Xue⁵, X.C. Yang⁷, Y. Yamamoto¹¹, Z.H. Ye¹⁴, G.C. Yu⁶, A.F. Yuan⁴, T. Yuda¹⁸, H.M. Zhang³, J.L. Zhang³, N.J. Zhang⁵, X.Y. Zhang⁵, Zhaxiciren⁴, and Zhaxisangzhu⁴

Abstract. Several strong TeV gamma-ray bursts were detected from Markarian 421 (Mrk 421) in the years 2000 and 2001 by the Tibet-III air-shower array at the statistical significance of 6.9 σ level. Mrk 421 was unprecedentedly active at X-ray and TeV gamma-ray energies during this period. The observed differential energy spectral index of the gamma-rays from Mrk 421 is $3.65\pm^{0.50}_{0.55}$ at energies from 2.6 TeV to 39 TeV, assuming a power law spectrum.

1 Introduction

A variable gamma-ray source Markarian 421 (Mrk 421) is a blazar class of active galactic nuclei (AGN) close to the BL Lac type object, at a redshift z=0.031. The angle of the jet axis blasting from Mrk 421 to the line of sight is considered to be very small. In 1991, EGRET detected gamma-ray emissions from Mrk 421, which was the first detection of an extragalactic gamma-ray source. The integrated pho-

Correspondence to: K. Kawata (kawata@icrr.u-tokyo.ac.jp)

ton flux above 100 MeV is $(1.4\pm0.3)\times10^{-7}~{\rm cm^{-2}~s^{-1}}$, and the differential photon energy spectrum is represented by a power law with an exponent of 1.96 ± 0.14 (Lin et al., 1992). Subsequently, detection of gamma rays at TeV energies from Mrk 421 was reported by the Whipple collaboration (Whipple). The average integral flux was measured to be $1.5\times10^{-11}~{\rm cm^{-2}~s^{-1}}$ above 0.5 TeV, corresponding to 0.3 times as large as that from the Crab Nebula, which often serves as the standard candle in TeV gamma-ray astronomy (Punch et al., 1992).

Occasionally, at TeV energies gamma-ray flux of Mrk 421 shows a rapid variability. The TeV observation of Mrk 421 by Whipple showed a significant variabilities on a few-hour time scale on May 14 and 15 in 1994, during which the average source flux above 250 GeV increased by approximately factor of ~10 (Kerrick et al., 1995). Such rapid variabilities of the TeV gamma-ray emissions were detected again by the Whipple from April 20 to May 5 in 1995 (Buckley et al., 1996) and May in 1996 (Gaidos et al., 1996) at sub-TeV energies. At the second outburst in 1996, which lasted approximately 30 minutes, the flux increased by a factor of

¹Department of Physics, Hirosaki University, Hirosaki, Japan

²Department of Physics, Saitama University, Saitama, Japan

³Laboratory of Cosmic Ray and High Energy Astrophysics, Institute of High Energy Physics, CAS, Beijing, China

⁴Department of Mathematics and Physics, Tibet University, Lhasa, China

⁵Department of Physics, Shangdong University, Jinan, China

⁶Institute of Modern Physics, South West Jiaotong University, Chengdu, China

⁷Department of Physics, Yunnan University, Kunming, China

⁸Faculty of Engineering, Kanagawa University, Yokohama, Japan

⁹Faculty of Education, Utsunomiya University, Utsunomiya, Japan

¹⁰Institute for Cosmic Ray Research, University of Tokyo, Kashiwa, Japan

¹¹Department of Physics, Konan University, Kobe, Japan

¹²Faculty of Systems Engineering, Shibaura Institute of Technology, Saitama, Japan

¹³Department of Physics, Yokohama National University, Yokohama, Japan

¹⁴Center of Space Science and Application Research, CAS, Beijing, China

¹⁵National Institute for Informatics, Tokyo, Japan

¹⁶Tokyo Metropolitan College of Aeronautical Engineering, Tokyo, Japan

¹⁷Shonan Institute of Technology, Fujisawa, Japan

¹⁸Solar-Terrestrial Environment Laboratory, Nagoya University, Nagoya Japan

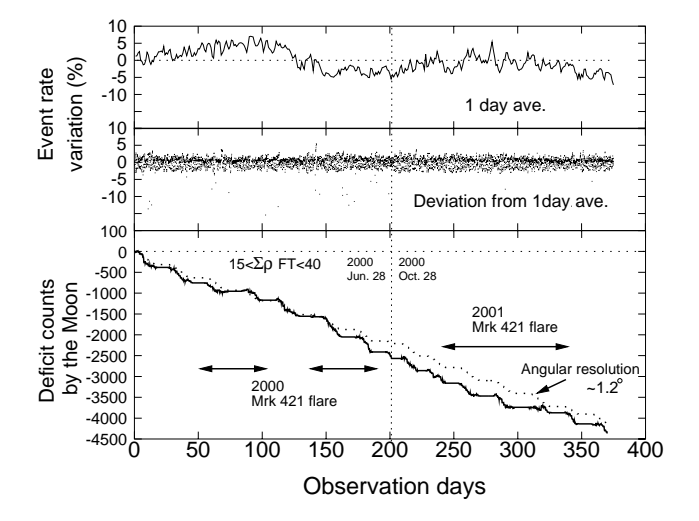


Fig. 1. Tibet-III long-term event rate stability in the upper figure, where the correction by the atmospheric pressure effect is not made. Also shown in the lower figure is the cumulative number of deficit events with $15 < \Sigma \rho_{\rm FT} < 40$ due to the Moon shadow for data (solid curve) and the expected assuming the angular resolution 1.2° (dotted curve).

20-25.

Then, Mrk 421 showed an increased X-ray and TeV gamma-ray activities in the year 2000 and the activities lasted until the year 2001 (ASM/RXTE web site., 2001). In this paper, we report on the results from data analysis of air shower events pointing back to the direction around Mrk 421 during its outbursting period in the years 2000 and 2001, using a large scintillation counter arrays (Tibet III) at Yangbajing in Tibet.

2 Experiment

An enlarged Tibet-III array, consisting of 533 scintillation counters which are placed at a lattice with 7.5 m spacing, has been operating with energy range around 3 TeV since 1999 at Yangbajing in Tibet, China (90.53°E, 30.11°N) at an altitude of 4,300 m above sea level, an atmospheric depth of 606 g/cm². Each counter has an area of 0.5 m², and plastic scintillators of 3 cm thickness and 2 inch diameter PMTs are equipped (Amenomori et al., 2001).

The mode energy of triggered air showers by the Tibet-III array is about 3 TeV, covering the upper part of the energies by the atmospheric Cherenkov technique. The energy of each primary particle is estimated from air shower size $\Sigma \rho_{\rm FT}$, where $\rho_{\rm FT}$ is the number of particles per m² observed in each detector and the summation is taken for all fired detectors. Triggering condition is any 4-fold coincidence of 0.8 particle within 300 ns gate width, and the event rate is about 680 Hz (Amenomori et al., 2001).

The amount of displacements of the Moon shadow are quite consistent with the geomagnetic deflection of mixed primary cosmic-ray protons with energy. The displacement of Moon shadow center in the north-south direction can give the systematic error of pointing the object at 0.1° level. The energy scale uncertainty is estimated to be less than $\pm 10\%$ level (Amenomori et al., 2001).

The long-term stability of the daily event rate is shown in Fig. 1, where its variation is less than $\pm 5\%$. The cumulative number of deficit events (15 $< \Sigma \rho_{\rm FT} < 40$) by the Moon shadow is shown also in Fig. 1 which demonstrates the detector pointing accuracy and the angular resolution is stable.

3 Event Selection and Data Analysis

The number of recorded shower events is about 4.3×10^9 for the period from Nov. 18 in 1999 to May 1 in 2001, during which the detector live time is 316.3 days. In order to extract an excess of TeV gamma-ray events coming from Mrk 421, the background event density has to carefully be estimated. According to the detector angular resolution estimated by the Moon shadow in Fig. 1, we set the following on-source angular cell centered at the source direction with a radius of 1.4° , 1.0° , 0.5° , and 0.4° for events with $15 < \Sigma \rho_{\rm FT} < 40$, $40 < \Sigma \rho_{\rm FT} < 100$, $100 < \Sigma \rho_{\rm FT} < 400$ and $400 < \Sigma \rho_{\rm FT} < 1000$, respectively, to optimize the S/N ratio.

The background is estimated by number of events averaged over 8 off-source cells with the same angular radius as on-source, at the same zenith angle, recorded at the same time intervals as the on-source cell events. The definite positions of these off-source cells, located at every 3.2° step from the source position measured in unit of angle distance in the azimuthal direction at the same zenith angle as the on-source direction, move picking up events incident always at the same time as the on-source cell moving on the sky with time.

It should be noted we exclude the two adjacent off-source cells to the on-source cell to avoid a possible signal tail in the off-source events. This method, so-called "equi-zenith angle background estimation", can estimate the background under the same condition as the on-source, however, it fails while the source object stays remarkably closes to the zenith, because the off-source cells overlap with the on-source cell. In fact, this method is applicable when the on-source object exists at the zenith angle larger than 8°. Fortunately, as the zenith angle of Mrk 421 at crossing the meridian is about 7° at Yangbajing, each on/off-source cell is independent throughout the observation period.

4 Results and Discussions

The statistical significance of TeV gamma-ray signal from Mrk 421 is calculated using the excess events

$$(N_{\rm on} - N_{\rm off})/\sqrt{N_{\rm off}},$$

where $N_{\rm on}$ and $N_{\rm off}$ are the number of events within the onsource cell and the number of events averaged over 8 offsource cells.

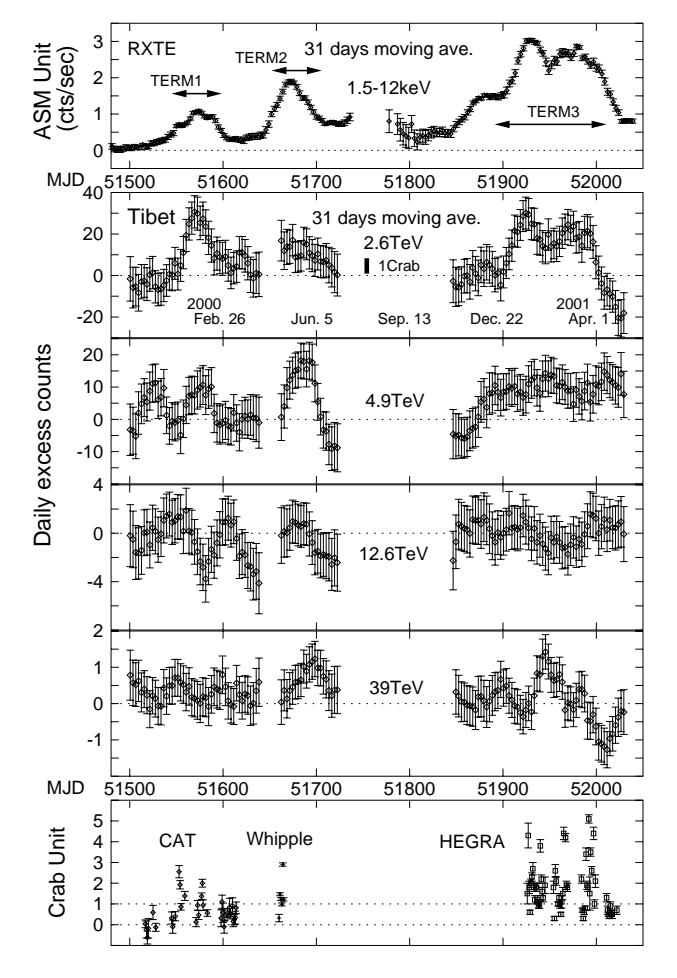


Fig. 2. 31-day moving average of the daily excess event rates around the Mrk 421 flaring period in the years 2000 and 2001, together with the RXTE X-ray satellite observation (ASM/RXTE web site., 2001). Also shown are the obsevations by Cherenkov Telescopes, CAT (Holder et al., 2000), Whipple (IAU Circulars., 2000), HEGRA (HEGRA web site., 2001).

We plot the 31-day and 7-day moving average of our daily excess event rate from Mrk 421 in Fig. 2 and Fig. 3, respectively, together with the Rossi X-Ray Timing Explorer (RXTE) (ASM/RXTE web site., 2001). We see an excellent correlation between them as shown in Fig. 2 and Fig. 3. Then, according to the flaring state of Mrk 421, the Tibet-III dataset is divided into 3 terms, as summarized in Table 1. The excess events in TERM 1+2+3 for the whole period are plotted on the equatorial coordinates as shown in Fig. 4, to demonstrate that a clear peak is observed in the Mrk 421 direction.

In order to calculate the energy spectrum of gamma rays from Mrk 421, the detector response of the Tibet-III array is simulated by a full Monte Carlo simulation using the Cosmos uv5.65 (Kasahara., 1995) air-shower generation code and the Epics uv6.60 (Epics web site., 2001) detector response code. To estimate the effective area of the detector, we generated gamma-ray events with a differential spectral index of -2.6, tracing the orbital motion of Mrk 421 on the atmosphere. The

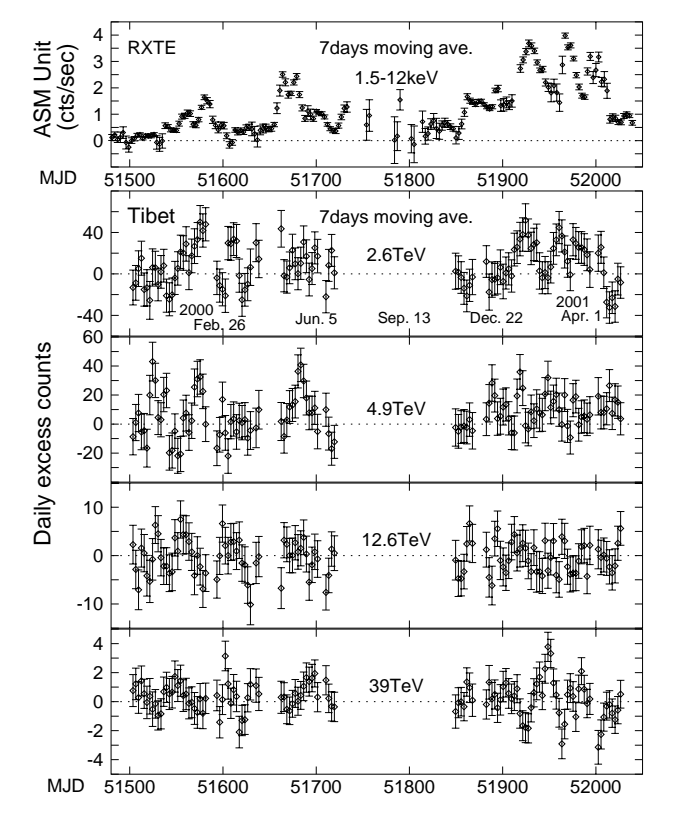


Fig. 3. 7-day moving average of the daily excess event rates around the Mrk 421 flaring period in the years 2000 and 2001, together with the RXTE X-ray satellite observation.

core location of an air shower generated by the event is uniformly distributed over an area centered at the array 300 m in radius which include the area where gamma-ray events are actually triggered in our array. Using the calculated effective area, the excess event rate, live time, and correlation between $\Sigma \rho_{\rm FT}$ and primary gamma-ray energy, the differential energy spectra corresponding to TERM 1, 2 and 3 are calculated as shown in Fig. 5. Each energy spectrum appears consistent within current statistics. Combining the 3 energy spectra together in Fig. 6, we obtain a differential energy spectrum with a spectral index of $-3.65\pm_{0.55}^{0.50}$, which is consistent with the observation -2.94 ± 0.06 in the year 2000 by HEGRA (Krowczynski et al., 2001). An extensive of study the systematic errors is now under way. The feature for which this flare was conspicuous is that the energy of observed gamma rays is extended to 40 or more TeVs. To understand the gamma-ray emission mechanism more deeply, one needs to make a continuous observation of Mrk 421 with better statistics.

TERM	MJD	Live Time (days)
1	51551 - 51599	40.5
2	51661 - 51705	38.9
3	51900 - 52012	91.6

Table 1. Definition of Mrk421 flaring terms in this analysis.

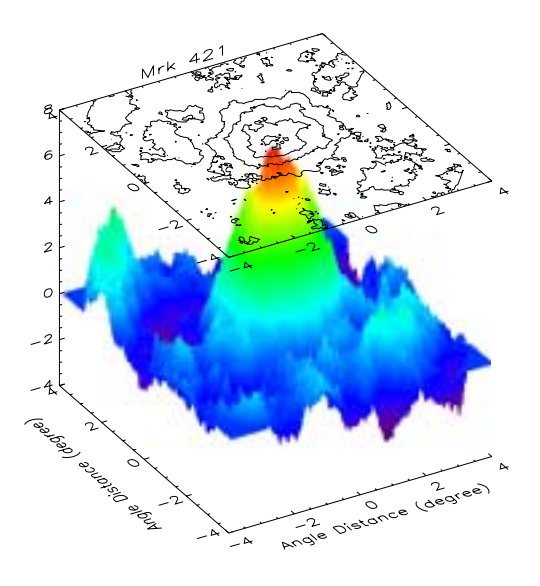


Fig. 4. 3D contour map of the weights of excess event densities around Mrk 421 in the area of $4^{\circ} \times 4^{\circ}$ centered at the direction of Mrk 421. Peak excess with 6.9 σ is seen at the center for TERM 1+2+3.

5 Summary

Coincident with the X-ray RXTE satellite observation, the Tibet-III array successfully detected the TeV gamma-rays, at the 6.9 σ statistical significance from Mrk 421 which were in a very active phase during the years 2000 and 2001.

Acknowledgements. This work is supported in part by Grants-in-Aid for Scientific Research and also for International Scientific Research from the Ministry of Education, Culture, Sports, Science and Technology in Japan and the Committee of the Natural Science Foundation and the Academy of Sciences in China.

References

Amenomori, M. et al., Talk given by M. Ohnishi at ICRC 2001, will be published in the proceedings.

ASM/RXTE team, http://xte.mit.edu/ASM_lc.html

Buckley, J.H. et al., ApJ, 472, L9 (1996)

Gaidos, J.A. et al., Nature, 383, 26 (1996)

HEGRA collaboration,

http://wpos6.physik.uni-wuppertal.de:8080/

Holder, J., astro-ph/0010264.

IAU Circulars, Circular No. 7414 (2000).

Kasahara, K., Proc. 24th ICRC, 1, 339 (1995),

http://eweb.b6.kanagawa-u.ac.jp/~kasahara/ResearchHome/cosmosHome/index.html

Kasahara, K., Epics web site.

http://eweb.b6.kanagawa-u.ac.jp/~kasahara/ResearchHome/EPICSHome/index.html

Kerrick, A.D. et al., ApJ, 438, L59 (1995)

Krowczynski, H. et al., astro-ph/0105331.

Lin, Y.C. et al., *ApJ*, **401**, L61 (1992)

Punch, M., Nature, 358, 477 (1992)

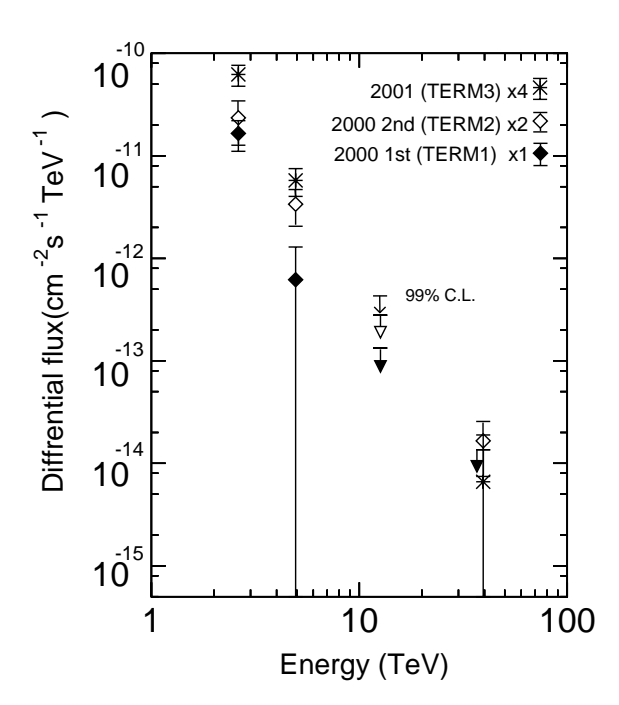


Fig. 5. Comparison of the differential spectrum of gamma rays from Mrk 421 obtained at the TERM 1, 2 and 3. The error bars indicate the 1 σ statistical ones, not the systematic ones, and the upper limits are given at the 99% confidence level. To avoid the overlapping among data points, the flux is multiplied by a factor of 2 and 4 for TERM 2 and 3, respectively.

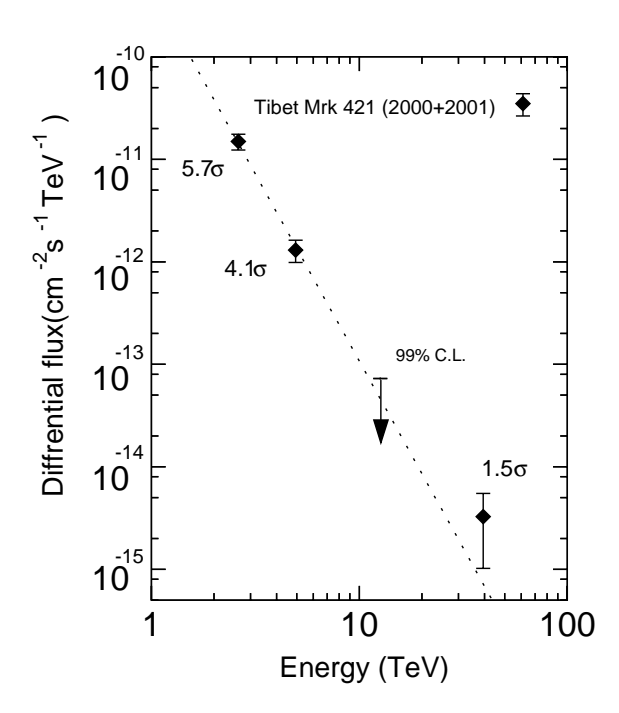


Fig. 6. Differential energy spectrum of the observed gamma rays from Mrk 421 averaged over the the flaring TERM 1+2+3. The error bars indicate the 1 σ statistical ones, not the systematic ones, and upper limit is given at the 99% confidence level.